



# Heavy Metals and Carbapenem-Resistant *Klebsiella pneumoniae* in a River System of Odisha, India: Correlation and Integrated Risk Assessment

Pragyan Paramita Swain<sup>1</sup> · Enketeswara Subudhi<sup>1</sup> · Rajesh Kumar Sahoo<sup>1</sup>

Received: 23 November 2024 / Accepted: 28 May 2025  
© The Author(s) 2025

## Abstract

The unregulated release of heavy metals and antibiotics into rivers has the potential to significantly impact human health. Infections caused by healthcare-associated pathogen, carbapenem-resistant *Klebsiella pneumoniae* (CRKP), present a critical challenge to clinical practitioners due to its resistance to last-line antibiotics. In this study, we investigated co-contamination of heavy metals (As, Cd, Cr, Mn, and Pb) and CRKP isolates in water samples from multiple sites along the river receiving wastewater discharge from urban areas of twin-city, Odisha. We used a composite risk scoring framework integrating chemical risks (based on hazard indices (HI) of heavy metals) and biological risks (based on the proportion of CRKP isolates exhibiting multidrug-resistant phenotypes and their multiple antibiotic resistance (MAR) index. Furthermore, Spearman's correlations and redundancy analysis (RDA) were employed to assess the association between heavy metals and antibiotic resistance genes (ARGs). From the total CRKP isolates identified ( $n = 91$ ), 90.1% and 9.89% exhibited multidrug resistant (MDR) and extensively drug-resistant (XDR) phenotypes, respectively. Sites D2 and C2 were flagged as high-risk sites based on their composite risk scores of 0.735 and 0.699, respectively. Positive correlations were observed between heavy metals and ARGs ( $bla_{OXA-48}$ ,  $bla_{TEM}$ , and  $bla_{SHV}$ ). The findings raise concern regarding the potential threat of CRKP and heavy metal pollution in river water while also emphasizing the need for integrated assessment to control their release into the environment.

**Keywords** Heavy metals · Carbapenem-resistant *Klebsiella pneumoniae* · Antimicrobial resistance · Risk assessment · Virulence · River water

## Introduction

River water plays a vital role in the functioning of ecosystems and offers essential services that benefit human well-being. However, the proper functioning of rivers is disturbed due to the impact of anthropogenic activities, thus affecting the surface water quality. The discharge of partially treated/untreated wastewater directly into the rivers has resulted in the release of heavy metals, antibiotics, and various opportunistic pathogens into the environment. Heavy metals (HMs) enter the river through both natural and

anthropogenic sources, including metals released from rock, animal farming, treated and untreated household wastes, urban runoff, mining and industrial discharges, and agricultural wastes [1, 2]. Certain heavy metals at low concentrations are crucial for various biological macromolecules and cellular processes; however, chronic exposure to increased HM concentrations has adverse outcomes on micro and macro organisms [3, 4]. Heavy metals like Cd, Pb, Cr, and As can cause nephrotoxicity and chronic kidney diseases, while excessive Mn has been linked to neurotoxicity [5]. Residual antibiotics persist in the environment, fostering the growth of antibiotic-resistant bacteria (ARB) and accumulation of antibiotic resistance genes (ARGs) which can be horizontally transferred to other pathogens, posing a significant health risk.

*Klebsiella pneumoniae* is a leading cause of hospital and community-acquired infections, such as pneumonia, urinary tract infections, wound infections, and bloodstream

✉ Rajesh Kumar Sahoo  
rajeshkumarsahoo@soa.ac.in

<sup>1</sup> Centre for Biotechnology, Siksha O Anusandhan (Deemed to Be University), Kalinganagar, Ghatikia, Bhubaneswar, Odisha 751003, India

infections, being listed as a priority pathogen by the World Health Organization (WHO) [6]. The rising incidence of carbapenem-resistant *K. pneumoniae* (CRKP) is associated with high mortality rates reaching up to 40–50% in non-native infections [7, 8]. Moreover, the spread of CRKP into the aquatic environments is particularly worrisome due to the risk posed to human health from exposure to the contaminated rivers [9]. Besides, HM contamination in the environment poses a substantial risk to the selection and emergence of ARB through co-resistance and cross-resistance mechanisms [10]. Recent studies have reported the emergence and persistence of antimicrobial resistance (AMR) in pathogens due to heavy metal contamination in the environment [11]. Resistance to antibiotics and heavy metals often co-exists on mobile genetic elements (MGEs) such as plasmids, integrons, and transposons that facilitate horizontal gene transfer (HGT) among bacteria. Such co-occurrence patterns have been reported in diverse environments, such as rivers, wastewater treatment plants, and areas associated with agricultural, industrial, and clinical activities [12]. Mechanisms such as overexpression of efflux pumps and reduced membrane permeability have been implicated in both antibiotic and heavy metal resistance [13]. Given this significant overlap between metal and antibiotic resistance mechanisms, studying the CRKP and heavy metal pollution in water systems may offer insights into potential associations relevant to antimicrobial resistance monitoring.

Antibiotic resistance is notably high in regions such as Africa and Southeast Asia mostly due to poor hygiene, insufficient healthcare facilities, and the absence of robust pollution control regulations [14]. Despite the growing concern, there remains limited research on the co-occurrence and spatial distribution of heavy metals and CRKP in river systems receiving urban wastewater. Importantly, there is a need to assess the spatial co-occurrence of these contaminants and their potential association that may support the persistence of ARGs. Therefore, in this study, we focused on two populated and urban twin cities in the eastern part of India, surrounded by over 500 hospitals, nursing homes, and clinics. We hypothesized that the co-occurrence of heavy metals and CRKP in wastewater-contaminated rivers may result in conditions conducive to ARG persistence. By using redundancy analysis (RDA) and integrating chemical (hazard indices) and biological risk assessments (MAR indices), we aim to explore their associations and provide novel insights into the public health risks associated with wastewater discharge into the riverine ecosystems.

## Methodology

### Description of the Study Area and Water Sample Collection

The Mahanadi River system is the third most extensive river system in Peninsular India, following the Godavari and Krishna rivers. It is also the largest river with an approximate length of 494 km in the state of Odisha. The sampling sites encompass the Mahanadi River and its tributaries (Kathajodi, Kuakhai and Daya), spanning two adjacent Tier-II cities in India, viz. Cuttack and Bhubaneswar (Fig. 1). Both cities are considered health capitals and industrial hubs of the eastern part of India, with an estimated population of 1.8 million. These cities are rapidly evolving metropolitan hubs, with Bhubaneswar (State capital of Odisha) specifically recognized as a Smart City under the Government of India's smart city project. The rivers Kathajodi, Kuakhai, and Daya serve as critical water sources for the twin city, supporting recreational activities, agriculture, and livestock farming. However, multiple reports highlight the severe public health concerns associated with these water bodies. Notably, contaminated water from the Daya river has been linked to an outbreak of acute diarrhea affecting over 90 people, with several deaths [15, 16]. These incidents underscore the urgent need to monitor and mitigate the environmental and public health risks posed by polluted river water.

The water samples were taken during the post-winter season March–April 2023, because it has low precipitation and minimal runoff, which reduces the dilution impact. This allows for a more precise characterization of the microbial population and resistance profile in the river system. The collection sites spanned a total distance of 70 km, covering both rural and urban areas. Between upstream and downstream, the midstream of the river system is exposed to human activities (also referred to as catchment areas) and received urban wastewater (including domestic wastewater, industrial wastewater, hospital wastewater, and sewage water) discharge.

Water samples in triplicates (one liter each) were collected 0.5 m below the river surface in a clean sterile amber glass bottle from nine sampling sites representing river water (C1: Mahanadi River; C3: Kathajodi river; C5: Kuakhai river; D1: Daya river; D3: Daya river at catchment; and D4: Daya at downstream) and urban wastewater (C2: wastewater discharge to Kathajodi; C4: wastewater discharge to Kuakhai; and D2: wastewater discharge to Daya) (Supplementary Table 1). Site C1 was chosen as the control site for all the rivers due to its minimal anthropogenic influence during water collection. A total of 27 water samples were collected, transported in cooling conditions to the laboratory, and processed for the physicochemical, metal, and bacteriological analyses on the same day of collection. The

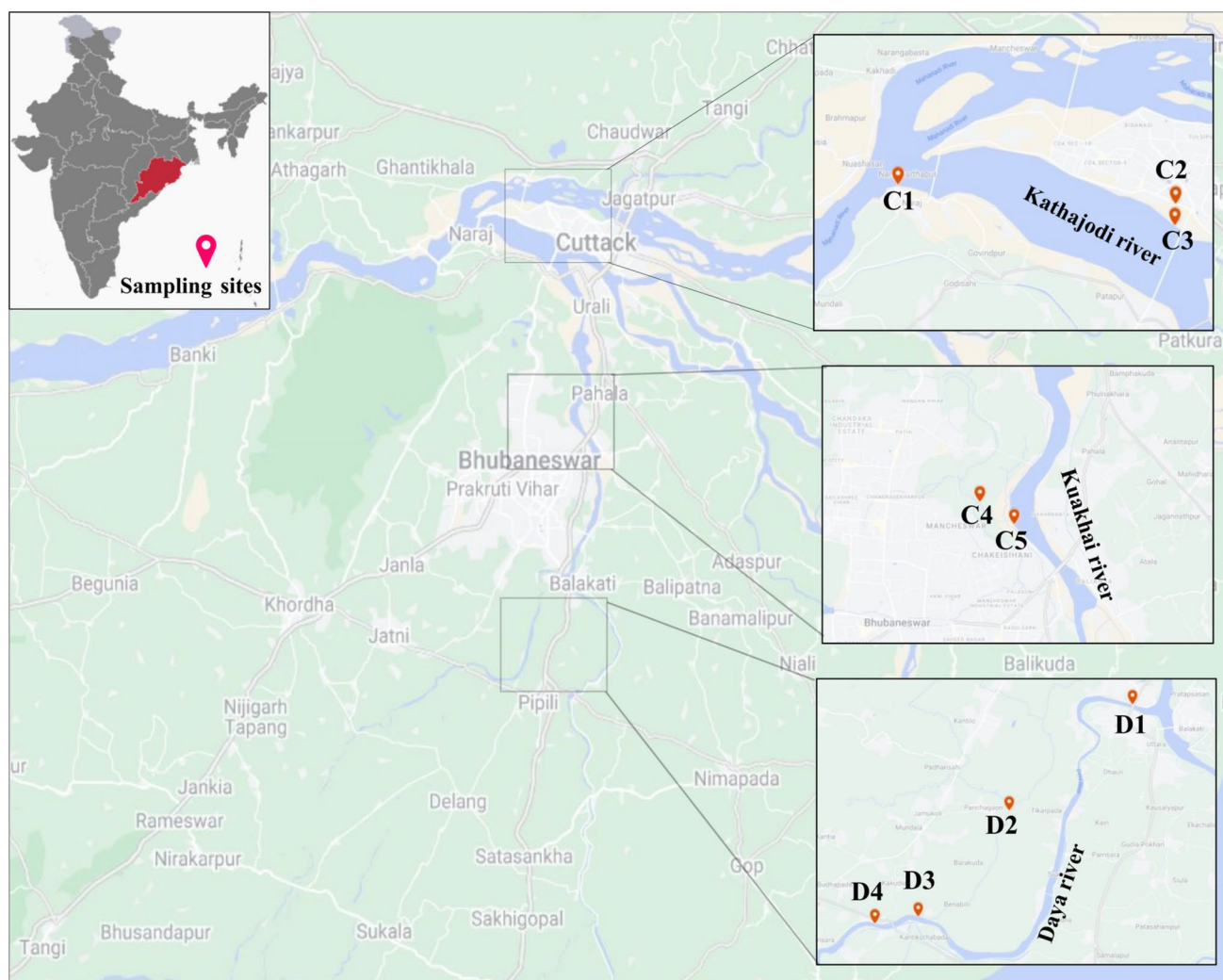


**Fig. 1** Map showing sampling sites (red color) across the distributaries of River Mahanadi encompassing the district of Cuttack and Bhubaneswar, Odisha, India

samples in triplicates were pooled as a single representative sample from each site.

### Physicochemical Parameters and Heavy Metal Composition Analyses

The water parameters, pH, and temperature were measured using a pH meter (Adwa AD12) and a digital thermometer (MT-222 Digiflexi, Dr. Morepen, India), respectively. Additional parameters, including Biological Oxygen Demand (BOD), Chemical Oxygen Demand (COD), and Dissolved Oxygen (DO) were assessed according to the guidelines provided by American Public Health Associations [17], and results were interpreted according to the United States Environmental Protection Agency (EPA) [18], WHO, and Bureau of Indian Standards (BIS) [19]. Furthermore, membrane

filtration technology was used to compute the total coliform (TC) and fecal coliform (FC) [17].

Heavy metals, namely, arsenic (As), cadmium (Cd), chromium (Cr), manganese (Mn), and lead (Pb), were analyzed using an inductively coupled plasma-optical emission spectrometer instrument (ICP-OES, USA) (Agilent 7700 × ICP-MS, USA). The results were interpreted according to the standard limits established by the EPA, WHO, and BIS.

### Heavy Metal Contamination Assessment

To understand the contamination of heavy metals in the surface water of the river system, contamination factor (Cf) and contamination degree (Cd) were measured by using Eq. (1) and (2) as described by Pobi et al. [20]. The Cf values  $< 1$ ,  $1 \leq Cf < 3$ ,  $3 \leq Cf < 6$ , and  $\geq 6$  are classified as having a low,

moderate, considerable, and very high level of contamination, respectively. Similarly, if the Cd values are  $< 8$ ,  $8 \leq \text{Cd} < 16$ ,  $16 \leq \text{Cd} < 32$ ,  $\text{Cd} > 32$ , they are classified as low risk, moderate risk, considerable risk, and high risk, respectively.

$$C_{fi} = C_i/B_i \quad (1)$$

$C_{fi}$  represents the contamination factor of the  $i$ th metal;  $C_i/B_i$  is the ratio of the measured concentration of metal in the water sample and the background value of the metal (mg/kg). The background concentration of heavy metals was determined as described by Husain et al. (2020). The concentration of heavy metals at Rajim, an upstream station in the Mahanadi River, was taken as the background values of heavy metals [21]

$$Cd = \sum_{i=1}^{i=n} C_f \quad (2)$$

The pollution load index (PLI) measures the cumulative metal pollution load in the study area by using Eq. (3). The obtained values were categorized as no pollution ( $\text{PLI} < 1$ ), moderate pollution ( $1 < \text{PLI} < 2$ ), heavy pollution ( $2 < \text{PLI} < 3$ ), and extremely heavy pollution ( $3 < \text{PLI}$ ).

$$\text{PLI} = (C_{f1} \times C_{f2} \times \dots \times C_{fn})^{1/n} \quad (3)$$

$C_{fn}$  represents the contamination factor of  $n$ th metal, and  $n$  is the number of metals.

## Human Health Risk Assessment

Humans are usually exposed to heavy metals through three major routes: ingestion, skin contact, and respiration. In this study, the risk to human health due to metal exposure through dermal contact and ingestion has been evaluated. The EPA computations were used to carry out the health risk evaluation where chronic daily intake (CDI) ingestion

and CDI dermal indicate the chronic daily intake of metals by ingestion and dermal adsorption using Eqs. (4) and (5), respectively [22, 23]

$$\text{CDI ingestion} = \left( \frac{IR \times EF \times ED}{BW \times AT} \right) C_w \quad (4)$$

$$\text{CDI dermal} = \left( \frac{SA \times ET \times K_p \times EF \times ED \times CF}{BW \times AT} \right) C_w \quad (5)$$

where  $IR$  is the ingestion rate per unit time (L/day),  $EF$  is the exposure frequency (days/year),  $ED$  is the exposure duration (years),  $BW$  is body weight (kg),  $AT$  is the average exposure time (days), and  $C_w$  refers to heavy metal concentration in water ( $\mu\text{g/L}$ ). The other variables are listed in Table 1.

The hazard quotient (HQ) was determined from CDI ingestion and CDI dermal exposure using Eqs. (6) and (7) as described by Imran et al. (2019).

$$\text{HQ ingestion} = \frac{\text{CDI ingestion}}{i\text{RfD}} \quad (6)$$

$$\text{HQ dermal} = \frac{\text{CDI dermal}}{d\text{RfD}} \quad (7)$$

where  $i\text{RfD}$  and  $d\text{RfD}$  refer to reference dose for ingestion and reference dose for dermal.

Table 1 represents the factors and assumptions used to estimate the exposure to heavy metals through ingestion and dermal absorption, explicitly focusing on their non-carcinogenic health impact.

Hazard index (HI) representing the potential non-carcinogenic risk of heavy metals ingested and absorbed dermally was evaluated for both adults and children by using the Eq. (8) [24, 25].  $\text{HI} > 1$  denotes probable adverse effects of metals on human health, and  $< 1$  denotes no adverse effect on human health.

**Table 1** Parameter used for calculating human health risk assessment through ingestion and dermal exposures

Parameters	Unit	Adult	Children
Ingestion rate (IR)	L/day	2	0.64
Exposure frequency (EF)	Days/year	365	365
Exposure duration (ED)	Years	70	6
Avg body weight (BW)	kg	70	20
Avg time (AT)	days	25550	2190
Skin area (SA)	$\text{cm}^2$	18000	6600
Exposure time (ET)	h/day	0.58	1
Permeability coefficient (Kp)	$\text{cm/h}$	0.002 for Cr; 0.001 for other metals	
Conversion factor (CF)	$\text{L/cm}^3$	0.001	
Reference dose (RfD)	$\mu\text{g/kg/day}$	Ingestion ( $i\text{RfD}$ ): As, 0.3; Pb, 1.4; Cr, 3; Mn, 20; Cd, 0.5 Dermal ( $d\text{RfD}$ ): As, 0.123; Pb, 0.42; Cr, 0.015; Mn, 0.8; Cd, 0.005	

$$HI = \sum_{i=1}^n HQ \quad (8)$$

### Isolation and Identification of CRKP Isolates

Water samples were passed through 0.22 µm (pore size) cellulosic membrane filter (Himedia, India) and the membrane was subsequently washed with 0.85% (w/v) NaCl solution. The eluant was serially diluted up to 10<sup>-3</sup> times, and dilutant (100 µL) spread on HiCrome™ *Klebsiella* Selective Agar Base (HiMedia) plate supplemented with meropenem (4 mg/L) and incubated at 37 °C for 24 h. The dark purple bacterial colonies (in the range of 30 to 300) were proceeded for further characterization. The DNA was extracted from overnight grown pure cultures of *Klebsiella* sp. using the modified Rapid One Step Extraction (ROSE) method [26]. Briefly, 1.5 mL of culture was centrifuged at 10,000 g for 10 min, and 500 µL of ROSE buffer was added to the pellet and mixed by pipetting. The mixture was incubated in a water bath at 85 °C for 1 h, followed by the addition of phenol to chloroform to isoamyl alcohol (PCI, 25:24:1) solution. After mixing the solution, it was further centrifuged for 10 min. The aqueous layer was transferred to another tube to which 2 volumes of chilled absolute ethanol was added, followed by incubation for 1–2 h at –20 °C. Following centrifugation for 5 min, the supernatant was discarded, pellet air dried and dissolved in 50 µL of T<sub>10</sub>E<sub>1</sub> buffer. The DNA quality and quantity were evaluated using agarose gel electrophoresis and Nanodrop™, respectively. All the carbapenem resistant *Klebsiella* sp. were further confirmed as *K. pneumoniae* (CRKP) through the amplification of the 16S-23S internal transcribed spacer (ITS) region and using *K. pneumoniae* ATCC13883 as a control strain. Polymerase chain reaction (PCR) was conducted in a 25 µL reaction mixture containing 12.5 µL of Taq PCR master mix (2X) (Qiagen, Germany), 1 µL each of forward and reverse primer (10 pM), 1 µL template (25 ng), and 9.5 µL of nuclease-free water. PCR conditions were as follows: initial denaturation at 94 °C for 3 min; 35 cycles of 94 °C for 1 min, 51.3 °C for 45 s, and 72 °C for 1 min; and a final extension at 72 °C for 10 min. Primers used in this study are listed in Supplementary Table 2.

### Molecular Typing of CRKP Isolates

The clonal relatedness of the CRKP isolates was determined using (GTG)<sub>5</sub>-PCR, a repetitive extragenic palindromic sequence-based PCR method [27]. The template DNA from CRKP isolates confirmed through ITS-PCR amplification was amplified using (GTG)<sub>5</sub> primer (Supplementary Table 2). The temperature profile for (GTG)<sub>5</sub>-PCR was as follows: 7 min of initial denaturation at 94 °C; 30 cycles of denaturation at 95 °C for 30 s, annealing at 45 °C for 1 min, and elongation at 65

°C for 8 min; and a final extension at 65 °C for 16 min. The unique fingerprinting pattern of the CRKP isolates and the identical fingerprinting pattern of isolates from different sites were selected for downstream analysis.

### Antimicrobial Susceptibility Study and Multiple Antibiotic Resistance (MAR) Index

The phenotypic screening for antimicrobial susceptibility of all CRKP isolates was performed by Kirby-Bauer disk diffusion test. The antibiotic disks and their concentrations used are mentioned in Supplementary Table 3. The polymyxin (colistin) resistance was tested by broth microdilution method as described by Das et al. [28]. The *E. coli* ATCC 25922 was used as a reference strain, and results were interpreted as per the Clinical & Laboratory Standards Institute (CLSI, 2020). Based on resistance phenotype, isolates were classified into either multi-drug resistant (MDR; resistant to at least one antibiotic in three or more classes of antibiotics) or extensively-drug resistant (XDR; resistant to at least one antibiotic in all but two or fewer antibiotic classes) categories [29]. The MAR index was calculated using the formula as mentioned by Singh et al. [30]:

$$\text{MAR index} = \frac{\text{No. of antibiotics to which the isolate was resistant}}{\text{Total number of antibiotics tested}}$$

### Molecular Detection of Resistance Genes

To determine the presence of carbapenem resistance genes (*bla*<sub>NDM</sub>, *bla*<sub>KPC</sub>, and *bla*<sub>OXA-48</sub>), extended-spectrum β-lactamases (ESBLs) (*bla*<sub>CTX-M</sub>, *bla*<sub>SHV</sub>, and *bla*<sub>TEM</sub>), and outer-membrane porins (*ompK35*, *ompK36*, and *ompK37*), PCR was carried out. The PCR reaction mixture and conditions were the same as mentioned for 16S-23S ITS in the “Isolation and Identification of CRKP Isolates” section. The annealing temperature and primer sequences are listed in Supplementary Table 2.

### Determination of Virulence Factors (VFs) and Virulence Index

The presence of genes encoding VFs such as siderophores (*ybtS*, *iroB*, *iucA*, *iutA*, and *entB*), host adherence (*fimH* and *mrkD*), capsule (*magA*), metabolite transporter (*peg344*), and capsular serotype K2 was detected by PCR. The primers with the annealing temperature of each gene are mentioned in Supplementary Table 2. The virulence index was calculated using the following formula:

$$\text{Virulence Index} = \frac{\text{Sum of all positive virulence genotype exhibited by the isolate}}{\text{Total number of virulence genes tested}}$$

## Data Analysis

Statistical analyses were performed using R (R version 4.3.2). The normality of the data was verified by a Shapiro–Wilk test (Supplementary Table 4). Differences in MAR indices were determined using a Kruskal–Wallis test followed by Dunn’s post hoc pairwise test with a Bonferroni correction for multiple comparisons.

To assess the genomic antibiotic resistance and virulence genes of each isolate, the presence and absence of genes were assigned a value of one and zero, respectively. Spearman’s rank correlation coefficients ( $r_s$ ) were computed to establish the relationship between water parameters, metals, and resistance genes, and their nullity was evaluated. Furthermore, redundancy analysis (RDA) was performed to assess the influence of heavy metals on ARGs. The concentrations of all heavy metals were taken as the constrained variables, and the abundance of ARGs ( $bla_{NDM}$ ,  $bla_{OXA-48}$ ,  $bla_{TEM}$ , and  $bla_{CTX-M}$ ) was taken as response variables. The analysis was done using scaled data, and statistical significance was tested using permutation tests ( $p < 0.05$ ).

The band profiles for each isolate obtained from (GTG)<sub>5</sub>-PCR were converted to a binary matrix (1 and 0), 1 representing presence and 0 indicating absence of a characteristic band. Pairwise distances were computed using Jaccard distance metrics in R’s *dist* function. Hierarchical clustering was performed on this computed distance matrix using the “*hclust*” function with the average linkage method. The optimal number of clusters was determined using the Gap Statistic method via the *fviz\_nbclust* function from the *factoextra* package, with 1000 bootstrap iterations. The dendrogram was visualized and annotated using the online iTOL v6 web server (<https://itol.embl.de>).

To study the association between MAR index and Virulence index for different sites, a scatter plot was generated using *ggplot2* in R. Each point on the plot represents a data point, showing how the MAR index corresponds to the Virulence index for that particular isolate.

Additionally, a composite risk score analysis for the sites was performed by combining the chemical (reflected by the HI from both ingestion and dermal pathways) and biological risk indicators (as represented by the MAR indices and MDR phenotype) from each site. Both variables were normalized to a scale of 0–1 and combined using equal weights (0.5 for each) to obtain a composite risk score for each site. The sites were then ranked based on the composite risk scores.

Equal weights were assigned based on the assumption that both variables contribute equally to the overall site risk, justified by their distinct roles in ecological and health concerns. It serves as a neutral approach, avoiding arbitrary prioritization without additional evidence. To test the robustness of this assumption, sensitivity analysis was conducted

using alternative weights for chemical and biological risks (0.3:0.7, 0.6:0.4). Spearman’s rank correlation coefficients were computed to assess rank stability. To further assess the relationship between the chemical and biological risks, a linear regression analysis was performed with the composite chemical risk as the independent variable and the composite biological risk as the dependent variable. To check for the robustness of the linear-model assumptions, a set of standard residual-diagnostic plots (residuals vs. fitted, Normal Q–Q, scale–location, Cook’s distance) was examined.

## Results

### Physiochemical and Microbiological Parameters of River Water

The distribution of water parameters is shown in Supplementary Table 5. Levels of pH, temperature, DO, BOD, and COD varied from 7.0 to 7.7, 22 to 25 °C, 1.74 to 11.87 mg/L, 0.64 to 6.42 mg/L, and 64 to 224 mg/L, respectively. The pH of all water samples was slightly alkaline. BOD levels were elevated in the catchment (C3 and D3) and downstream (D4) sites of the river system, with the highest value at the C2 site. COD levels were elevated in all sites, exceeding the international standard limit (WHO, 2011). DO plays a vital role in supporting aquatic life in surface waters and had the highest value in the upstream region (C1) and the lowest value in the midstream of the Daya river (D3) where wastewater from Bhubaneswar city is discharged via Gangua Nallah (D2). The lower DO values indicate its consumption for organic matter oxidation. The TC and FC count in all water samples exceeded > 200 colonies, indicating the water unfit for human consumption.

### Heavy Metal Distribution in River Water

Table 2 summarizes the average concentrations of metals in the water samples from the study sites. The concentrations of heavy metals including As, Cd, Cr, and Pb at all sites were within the prescribed limit as per EPA, BIS, and WHO, whereas the concentration of Mn exceeded recommended guidelines Table 2. The mean heavy metal concentrations of the water samples followed the decreasing order  $Mn > Cr > As > Pb > Cd$ , with the highest mean value of 273.851 mg/L for Mn and lowest of 0.101 mg/L for Cd. The highest concentrations of Cr and Pb were found at the D3 site where wastes from Bhubaneswar city are discharged from Gangua nallah (D2). Mn concentration was highest in the downstream Daya river (D4). Cd had the highest value recorded at the site where Cuttack city effluent (C2) gets discharged into Kathajodi river (C3). All the metals had their

**Table 2** Metal concentration across sampling sites and relevant standards for metals in water

Metals (µg/mL)	Sampling sites										Recommended limits (µg/mL)			
	C1	C2	C3	C4	C5	D1	D2	D3	D4	BIS	WHO	EPA		
As	3.567 ± 0.012	3.965 ± 0.045	5.474 ± 0.063	4.449 ± 0.018	5.222 ± 0.057	0.446 ± 0.122	7.439 ± 0.011	5.287 ± 0.029	6.978 ± 0.103	10	10	10		
Cd	0.002 ± 0.000	0.544 ± 0.014	0.063 ± 0.003	0.065 ± 0.002	0.052 ± 0.003	0.004 ± 0.001	0.026 ± 0.003	0.061 ± 0.003	0.09 ± 0.003	3	3	5		
Cr	2.873 ± 0.006	11.04 ± 0.082	0.443 ± 0.008	0.354 ± 0.005	1.018 ± 0.005	9.896 ± 0.011	16.41 ± 1.366	8.891 ± 0.012	11.33 ± 0.051	50	50	100		
Mn	4.159 ± 0.017	370.6 ± 0.458	316.1 ± 0.987	190.1 ± 0.138	276.3 ± 0.201	277.7 ± 0.326	326.1 ± 0.603	386.2 ± 0.082	317.4 ± 0.148	100	NG	50		
Pb	0.034 ± 0.003	0.254 ± 0.005	0.0142 ± 0.001	0.01 ± 0.005	0.037 ± 0.002	0.184 ± 0.002	0.491 ± 0.007	0.343 ± 0.004	0.344 ± 0.020	10	10	NG		

BIS Bureau of Indian Standards, WHO World Health Organization, EPA Environmental Protection Agency, NG not given, mean ± standard deviation

lowest concentration values detected in the upstream Mahanadi River (C1).

## Heavy Metal Contamination and Risk Assessment

The results indicated that the surface water at all sites has a moderate and considerable degree of pollution due to Mn ( $1 \leq CF < 6$ ) (Fig. 2a, b). The PLI values represent the status of comprehensive pollution caused by heavy metals and showed sites C2, D2, D3, and D4 as heavily polluted ( $2 < PLI < 3$ ) (Fig. 2c).

The health risk assessment was determined to estimate the non-carcinogenic risk of toxic metals including As, Cd, Cr, Mn, and Pb in both children and adults. The hazard quotient  $HQ_{\text{ingestion}}$  and  $HQ_{\text{dermal}}$  for both adults and children are mentioned in Supplementary Table 6. It is important to note that  $HQ_{\text{ingestion}}$  and  $HQ_{\text{dermal}}$  of As, Cd, Cr, Mn, and Pb in both children and adults were under the acceptable range of 1. However, the  $HI_{\text{ingestion}}$  values of all heavy metals detected at sampling sites ranged from 0.374 to 1.342 for adults and 0.635 to 1.503 for children (Fig. 2d). The  $HI_{\text{dermal}}$  values ranged from 0.0337 to 0.2339 and  $1.13E-05$  to 5.474 for adult and children, respectively. The  $HI > 1$  in sites C2, C3, C5, D2, D3, and D4 indicates high health risk on long-term exposure to the metals in these sites.

## Identification and Genetic Relatedness of CRKP Isolates from Various Sites

A total of 332 isolates identified as *Klebsiella* spp. were obtained from HiChrome *Klebsiella* Agar (Himedia) plate supplemented with meropenem. Among them, 217 (C2,  $n = 30$ ; C3,  $n = 17$ ; C4,  $n = 38$ ; C5,  $n = 25$ ; D1,  $n = 24$ ; D2,  $n = 30$ ; D3,  $n = 28$ ; and D4,  $n = 25$ ) were identified as *K. pneumoniae* (65.36%) by amplification of 16S-23S ITS-Kp gene. Following GTG<sub>5</sub>-PCR screening, 91 distinct clones of CRKP isolates (C2,  $n = 18$ ; C3,  $n = 7$ ; C4,  $n = 26$ ; C5,  $n = 12$ ; D1,  $n = 8$ ; D2,  $n = 8$ ; D3,  $n = 7$ ; and D4,  $n = 5$ ) were obtained from all sites. The highest number of unique CRKP clones was obtained from Gangua nallah of Cuttack city (C4) and the least from downstream Daya river (D4). No CRKP isolates were obtained from the upstream Mahanadi River. The phylogenetic tree depicting the genetic diversity of 91 CRKP isolates was divided into nine optimal clusters (Fig. 3). The CRKP isolates identified from wastewater sites were found to cluster together with the isolates obtained from river water, indicating high clonal relatedness among the isolates. In cluster 4, we observed the CRKP isolates from wastewater C2, C4, and D2 as phylogenetically similar to river water C3, C5, D1, D3, and D4. Likewise, in cluster 6, isolates from wastewater C4 were phylogenetically similar to river water C3, C5, and D3.

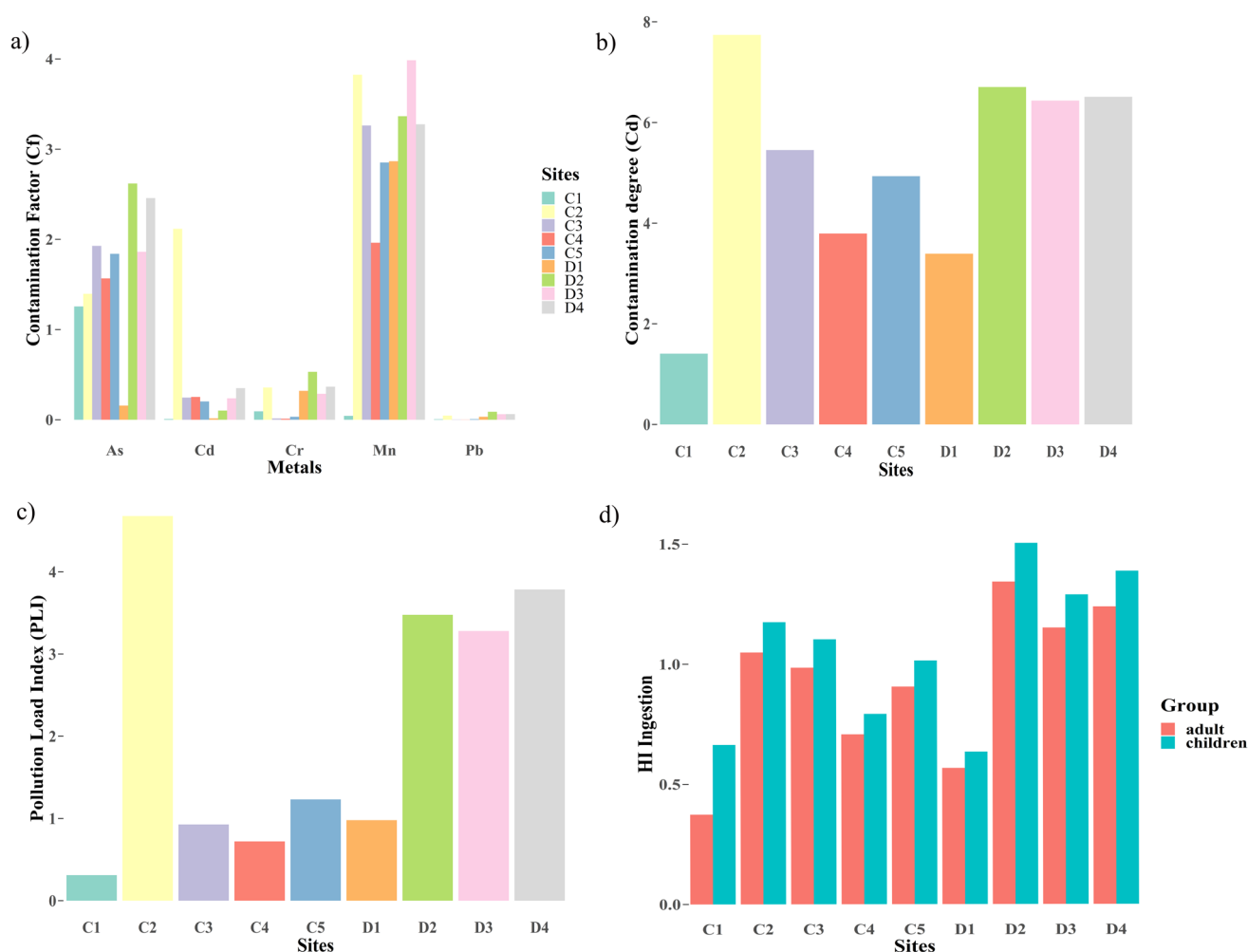


**Fig. 2** **a** Contamination factor (Cf); **b** Contamination degree (Cd); **c** Pollution load index (PLI); **d** Hazard index (HI) of heavy metals in different sampling sites

### Antimicrobial Susceptibility and MAR Index

Based on the resistance profile, 90.1% ( $n = 82$ ) of the isolates were classified as MDR, and the rest 9.89% ( $n = 9$ ) as XDR (Supplementary Table 3). The CRKP isolates exhibited complete resistance (100%) to piperacillin (PI), piperacillin-tazobactam (PIT), amoxicillin-clavulanic acid (AMC), meropenem (MRP), and imipenem (IMP) (Supplementary Fig. 1). Resistance rates exceeding 70% were also found against the following antibiotics: ceftriaxone (CTR) (91.2%,  $n = 83$ ), aztreonam (ATM) (87.91%,  $n = 80$ ), nalidixic acid (NA) (82.41%,  $n = 75$ ), trimethoprim-sulfamethoxazole (SXT) (80.21%,  $n = 73$ ), nitrofurantoin (N) (80.21%,  $n = 73$ ), tetracycline (TE) (78%,  $n = 71$ ), amikacin (AK) (76.92%,  $n = 69$ ), azithromycin (AZ) (75.82%,  $n = 69$ ), ciprofloxacin (CIP) (74.72%,  $n = 68$ ), ceftazidime (CAZ) (73.62%,  $n = 67$ ), and fosfomycin (FOS) (73.62%,  $n = 67$ ). Among the 91 CRKP isolates, 4.39% exhibited resistance to colistin, while all were susceptible to tigecycline. The isolates from

wastewater site C2 had the highest MAR index (0.84), followed by Daya river, D1 (0.75), and wastewater D2 (0.744) (Fig. 4a).

The average MAR indices of the sites differed from each other. A Kruskal–Wallis test gave a value of test statistic 19.7089 with  $p = 0.01$  indicating a significant difference between at least two groups in terms of MAR index. Pairwise multiple comparisons by Dunn's method revealed a significant difference in MAR indices ( $p < 0.05$ ) between site D3 and C2.

### Molecular Detection and Prevalence of Resistance Genes

Figure 4b displays the prevalence of resistance genes in CRKP isolates across the sample sites. The  $bla_{NDM}$  gene was identified in 68.13% of isolates, followed by  $bla_{OXA-48}$  (67.03%). The carbapenemase genes  $bla_{IMP}$ ,  $bla_{VIM}$ , and  $bla_{KPC}$  were not detected. Furthermore, 46.15% ( $n = 42$ )

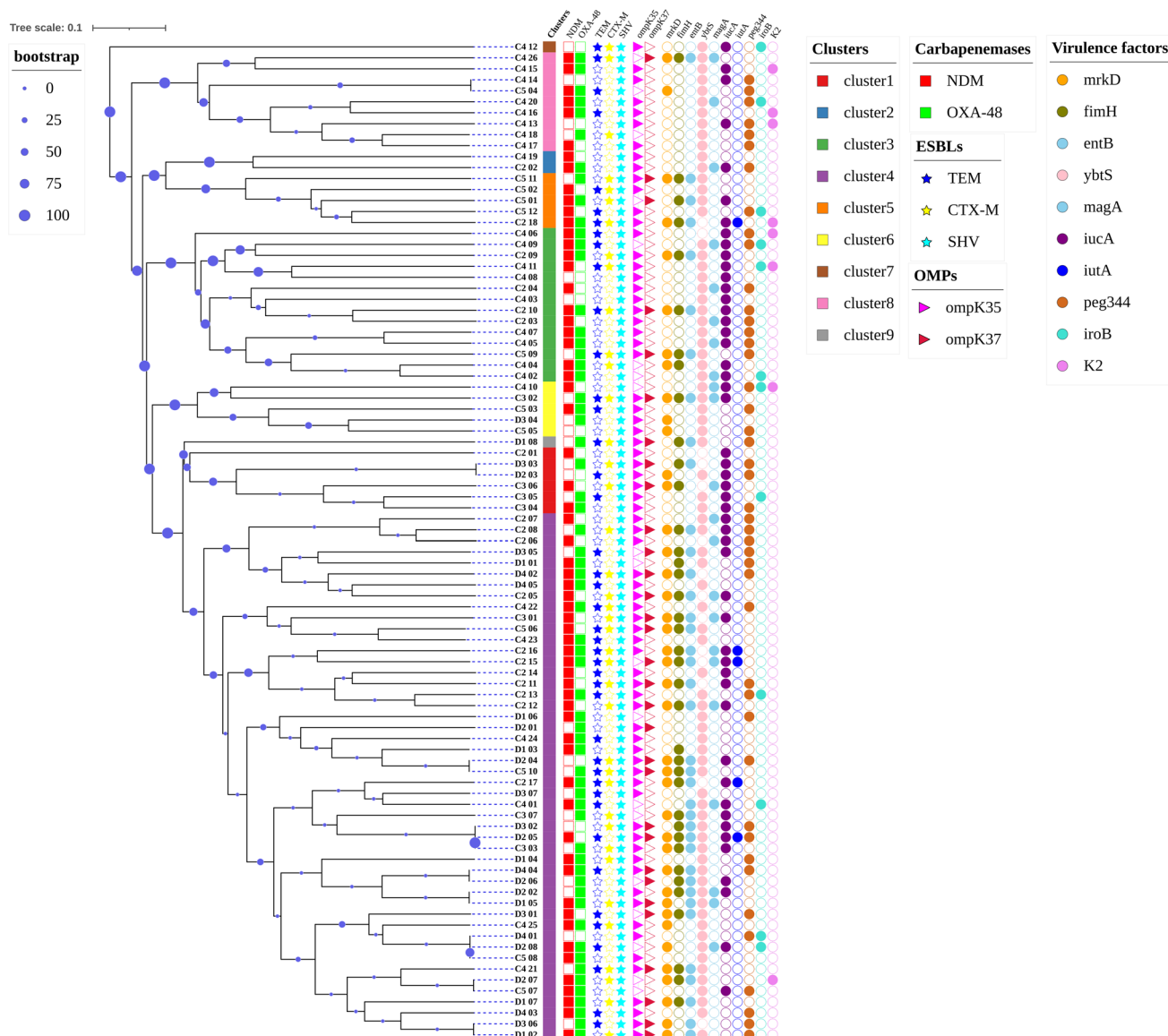


**Fig. 3** Heatmap supported by hierarchical clustering (dendrogram) based on (GTG)<sub>5</sub>-PCR fingerprints of CRKP isolates ( $n = 91$ ) depicting the distribution of carbapenemases, extended-spectrum  $\beta$ -lactamases (ESBLs), outer membrane porins (OMPs), and viru-

lence genes. Colors in the filled shapes indicate the presence of genes. The CRKP isolates belonging to clusters ( $n = 9$ ) were visualized as a color strip

isolates harbored both *bla*<sub>NDM</sub> and *bla*<sub>OXA-48</sub> genes. The maximum prevalence of *bla*<sub>NDM</sub> harboring isolates was obtained from wastewater samples at CDA, Cuttack (C2, 94.44%), followed by Daya river at midstream (D1, 87.5%) and downstream (D4, 80%). Similarly, the presence of *bla*<sub>OXA-48</sub> was detected in 100% of the isolates from D1, followed by D4 (80%). In sites C3 and D3, which receive wastewater from C2 and D2, *bla*<sub>OXA-48</sub> was found in 71.42% of the isolates. The co-resistance gene *bla*<sub>SHV</sub> was identified in all isolates, while *bla*<sub>TEM</sub> and *bla*<sub>CTX-M</sub> were present in 46.15% and 42.85% of isolates, respectively. Most genes *bla*<sub>NDM</sub>, *bla*<sub>TEM</sub>, and *bla*<sub>OXA-48</sub> (80%) were found to have

their highest prevalence in isolates from downstream Daya river (D4). Furthermore, the outer membrane porin (OMP) encoding genes *ompK35* (79.12%) and *ompK37* (34.06%) were abundant; however, *ompK36* was not detected in any of the isolates.

### VF and Virulence Index

The VFs encoding genes *mrkD*, *fimH*, *entB*, *ybtS*, and *peg344* were prevalent in CRKP isolates from all tested water sources (Fig. 5a). More than 50% of isolates from wastewater (C2, D2) and river water (C3, C5, D3, D4)

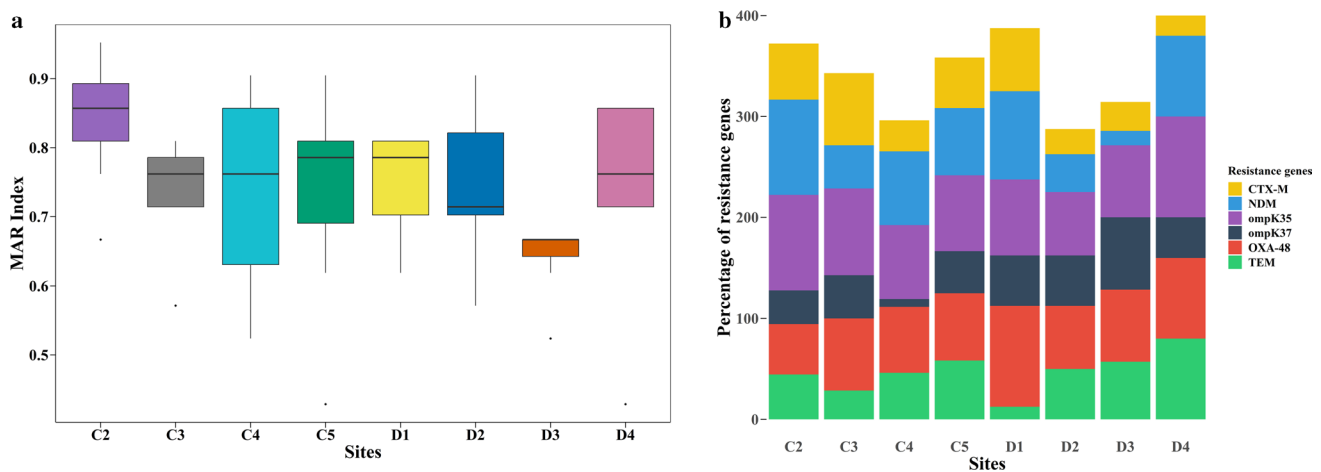


**Fig. 4** **a** Box plots representing average multiple antibiotic resistance (MAR) index of isolates from sites C2 to D4. **b** Stacked bar graph showing percentage resistance genes found in CRKP isolates across sample sites C2 to D4

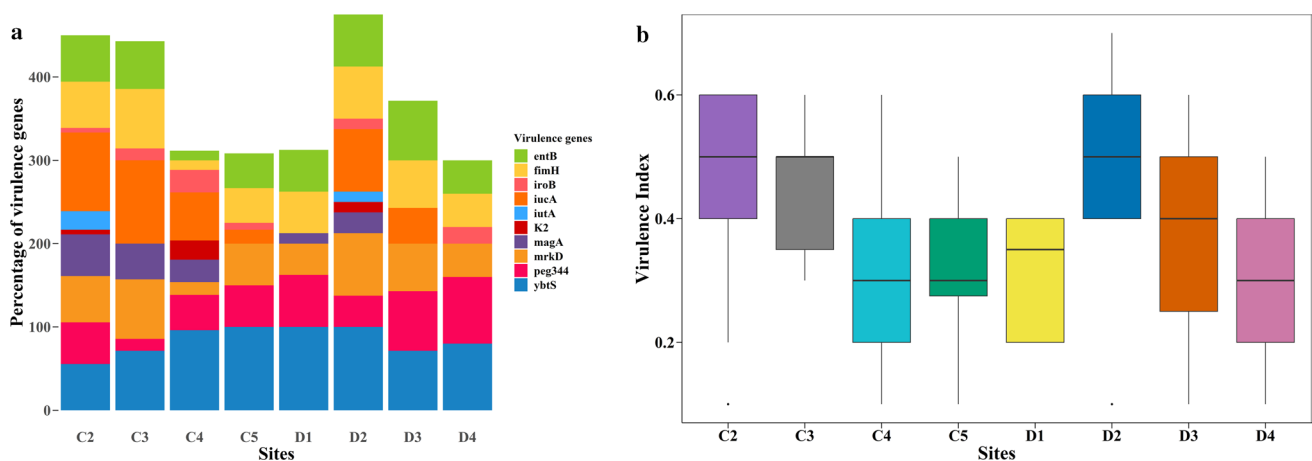


**Fig. 5** **a** Stacked bar graph showing percentage virulence genes found in CRKP isolates by sample sites C2 to D4. **b** Box plots representing average Virulence Index of isolates from sites C2 to D4

harbored *mrkD*, *fimH*, *entB*, *ybtS*, and *peg344* virulence genes. The *ybtS* gene was present in all isolates from sites C5, D1, and D2. A higher abundance of *iucA* and *magA* was found in isolates from C2, which discharges wastewater into the Kathajodi river (C3). The presence of the *iutA* gene was found only in the wastewater samples C2 (22.22%) and D2 (12.5%), while the *iroB* gene was detected in both wastewater (C2, 5.56%; C4, 26.92%; and D2, 12.5%) and river water (C3, 14.24%; C5, 8.33%; and D4, 20%).

The capsular serotype K2, however, was exclusively detected in CRKP isolates obtained from wastewater samples (C2, 5.55%; C4, 23.07%; D2, 12.5%). The average virulence index (VI) of all isolates was 0.36 and the maximum VI (0.475 and 0.45) was found in wastewater (D2 and C2), whereas the minimum VI (0.3) was observed in downstream Daya river (D4) (Fig. 5b). The Kruskal–Wallis test revealed

significant differences (test statistic = 18.633,  $p = 0.01$ ) in VI across the sites. The virulence index between sites C2 and C4 showed a notable significant difference (adjusted  $p = 0.0372$ ), indicating that the virulence characteristics in isolates between these two sites are statistically distinct.

### Risk Assessment of CRKP Isolates Transmitted from Wastewater to Rivers

We examined the link between MAR indices and virulence indices to estimate the public health risks of these isolates (Supplementary Fig. 2). Resistance levels are usually assessed using a MAR index of 0.2, following prior research [31]. However, the average MAR index across our study sites was 0.753, indicating stronger resistance in our isolates, which is a potential threat to

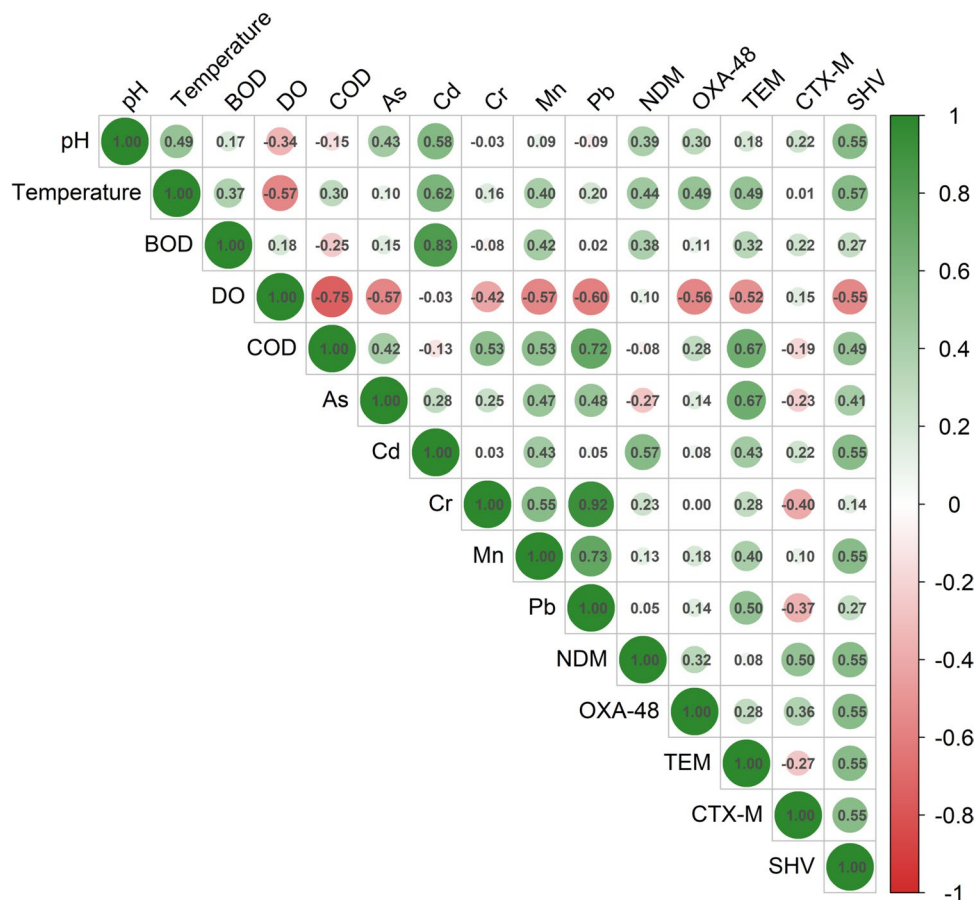
public health. Based on this, the isolates from site C2 were found to be of high potential threat as the MAR index  $\geq 0.753$  and the VI  $\geq 0.367$  (used as reference threshold based on the average virulence index across all sites in this study). Sites C3, D2, and D3 had VI  $\geq 0.367$  but MAR index  $< 0.753$ , indicating potential pathogenicity despite lower resistance. This helps comprehend the health concerns of antibiotic-resistant isolates in diverse areas and emphasizes the need for tailored interventions based on dual assessment of antimicrobial resistance and virulence.

Our analysis between MAR index and VI revealed varying degrees of association with the Spearman correlation coefficients ranging from 0.621 (suggesting a moderate positive association between the indices in D2 site) to  $-0.674$  (in site D3 indicating a moderate negative association). All sites showed a positive association between the MAR index and the Virulence index, except for sites C4 and D3, which showed a negative association. Although not statistically significant ( $p > 0.05$ ), these correlations highlight a complex interaction between virulence traits and antimicrobial resistance in different environmental conditions.

### Correlation Between Physicochemical Parameters, Metals, and Resistance Genes

The analyzed parameters of five physicochemical characteristics of the water (pH, temperature, DO, BOD, and COD), five metals in the surface water (As, Cd, Cr, Mn and Pb), two carbapenem-resistant genes (*bla*<sub>NDM</sub> and *bla*<sub>OXA-48</sub>) and three co-resistance genes (*bla*<sub>CTX-M</sub>, *bla*<sub>TEM</sub> and *bla*<sub>SHV</sub>) were used to construct a Spearman correlation matrix (Fig. 6). All metals showed negative correlation with DO. Most metals (As, Cr, Mn, and Pb) positively correlated with COD and Pb showed a significant positive correlation with COD ( $p < 0.05$ ). Pb correlated positively with all metals, particularly Mn ( $p < 0.05$ ) and Cr ( $p < 0.05$ ). COD showed a strong negative correlation with DO ( $p < 0.05$ ). The increased COD and reduced DO values indicate significant organic matter pollution in the water. COD has a strong positive correlation with *bla*<sub>TEM</sub> ( $p < 0.05$ ). All metals positively correlated with *bla*<sub>OXA-48</sub>, *bla*<sub>TEM</sub>, and *bla*<sub>SHV</sub> genes. As, Cr, and Pb showed negative correlation with *bla*<sub>CTX-M</sub>. Spearman's correlation between ARGs and heavy metals in river water showed that *bla*<sub>TEM</sub> was strongly correlated to As ( $p < 0.05$ ). The RDA explained 91% of the total variance in ARG distribution due to heavy metals collectively

**Fig. 6** Spearman correlation analysis between water parameters, heavy metals concentration, and ARGs features in CRKP isolates. The colors represent the correlation coefficient (red and green colors indicating negative and positive correlations, respectively). The strength of the color represents the numerical value of the correlation coefficient



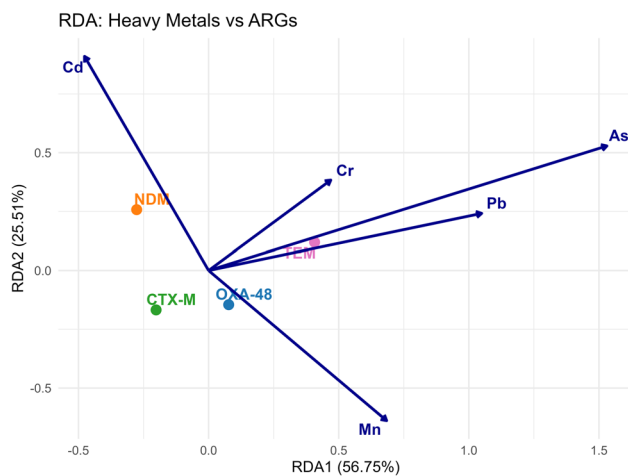


**Fig. 7** Redundancy analysis (RDA) plot showing the relationship between heavy metals and ARGs in studied sites. The arrows represent heavy metal concentrations, while the points correspond to ARG profiles across different sites. The direction and length of the arrows indicate the strength and influence of heavy metals on the distribution of ARGs

**Table 3** Composite risk score analysis of sites

Sites	Composite chemical risk	Composite biological risk	Composite risk score	Rank
D2	0.750023	0.719811	0.734917	1
C2	0.537138	0.861	0.699069	2
C3	0.594879	0.763208	0.679043	3
D4	0.626117	0.678302	0.65221	4
D3	0.557316	0.720755	0.639035	5
C5	0.291321	0.641755	0.466538	6
D1	0.19657	0.685731	0.441151	7
C4	0.153465	0.64666	0.400062	8
C1	0.008374	0	0.004187	9

(total inertia = 0.03703; constrained inertia = 0.033702). The effect size of each explanatory variable is visually represented by the length of their respective vectors. It is quantified as the Euclidean norm of their scores on RDA1 and RDA2 axes. RDA1 explains 56.75% of the total variance, while RDA2 explains 25.51% of it. As showed the strongest influence on the variation in ARGs with an effect size of ~0.81 followed by Pb (~0.54), Cd (~0.51), Mn (~0.47), and Cr (~0.30). The RDA model was statistically significant based on permutation testing ( $F = 4.0513$ ,  $p = 0.037$ , 999 permutations) (Fig. 7). In line with these findings, the composite chemical risk, composite biological risk, and overall composite risk scores for each site are presented in Table 3. Sensitivity analysis indicated high correlation ( $\rho = 0.9$ ) between equal weighted and alternative weighted composite scores, suggesting results are not sensitive to minor

variations in weighing (Supplementary Table 7). Notably, the linear regression model indicated a significant positive relationship between composite chemical risk and composite biological risk ( $p = 0.0438$ ,  $R^2 = 0.4627$ ). The intercept was estimated at 0.3630 (95% CI [0.0594, 0.6665]), and the slope at 0.6596 (95% CI [0.0243, 1.2948]). The standard residual diagnostics indicated approximate normality of residuals (Shapiro–Wilk,  $p = 0.37$ ) but showed evidence of heteroscedasticity (Breusch–Pagan,  $p = 0.03$ ) and one influential outlier (Bonferroni,  $p = 0.003$ ).

## Discussion

Anthropogenic activities have significantly impacted urban rivers by their widespread release of industrial wastes, domestic household effluents, hospital effluents, and untreated wastewater containing antibiotics, heavy metals, biocides, and pesticides into the water bodies. This has resulted in the proliferation and dissemination of ARBs and ARGs, negatively impacting human health and the environment. The present study examines the potential health hazards linked to the heavy metals and CRKP contamination resulting from the release of wastewater into the river and understanding the relationship between the water parameters, metal concentration in water, and abundance of ARGs in the CRKP isolates. The high BOD and low DO values in the river indicate significant domestic sewage contamination, suggesting substantial pollution levels, rendering the river water in the twin city unsuitable for drinking or domestic use. Similarly, high COD values observed in our study sites may be due to partially treated sewage and industrial effluents getting discharged into the river [32]. Although C1 was selected as a control site due to its distance from major urban discharge points, we acknowledge its limitations as a pristine reference. The elevated COD level in C1 may suggest minor anthropogenic influences such as the presence of organic pollutants primarily originating from agricultural activities in the vicinity, as well as algal-derived organic matter. Agricultural runoff can transport organic compounds from crop residues, fertilizers, and animal manure into the river. Additionally, the decay of algal material releases substantial amounts of cellular debris, which subsequently accumulates and undergoes decomposition [33]. All the water samples in the current investigation were found to be contaminated with coliform bacteria, including TC and FC, and their levels were above the recommended value set by the WHO. The presence of FC in river water indicates contamination by fecal material from both human and animal sources. According to Joshi and Mishra (2017), the contamination of Kuakhai river and Daya river with FC bacteria is owing to the discharge of untreated wastewater, sewage water, and open yard defecation still in practice along the riverside [34].

The contamination factor (Cf) indicated that the river water is highly contaminated with As and Mn heavy metals. The catchment (C3, C5, and D3) and downstream (D4) sites were moderately contaminated by As and Mn with the highest PLI. This may be due to anthropogenic activity in the Kuakhai river (C5) and Daya river (D3 and D4), where the total untreated wastewater and domestic wastes produced in the cities are directly discharged into the river through the main drainage system. Thus, the presence of metals can be attributed to the discharge of municipal and domestic wastes, excessive runoff of fertilizers from agricultural regions, or certain small-scale industries [35]. The Bhubaneswar city contained 88 industries, 34 of which are susceptible to directly contaminate the nearby rivers. The liquid wastes, consisting of wastes from residential, biomedical, and industrial wastes, are connected to Gangua Nala (C3 and D2), which is discharged to Kuakhai river (C5) and Daya river (D3 and D4) [34].

Based on  $HQ_{\text{ingestion}}$ , the potential health hazards due to exposure to As, Cd, Cr, Mn, and Pb are often higher for children compared to adults. In addition, the  $HI_{\text{ingestion}}$  values for adults and children at river sites (D3 and D4) were higher than 1, indicating that both adults and children are prone to experience adverse health risks from ingesting river water at these sites. The findings of our study are consistent with similar studies conducted on surface waters polluted with heavy metals in Egypt [36]. Children had high HI values compared to adults, suggesting a greater chance of non-cancer risks posed by heavy metals to children. This outcome aligns with previous studies conducted in Bangladesh [37] and Iran [38], which reported elevated HI values and associated health risks among children exposed to contaminated water.

The high genetic heterogeneity among CRKP isolates from various water sources was revealed through (GTG)<sub>5</sub>-PCR fingerprinting. The isolates from wastewater sites (C2, C4, and D2) showed clonal similarity to those from river water sites (C3, C5, D1, D3, and D4), indicating potential dissemination from wastewater to the river. This observation is consistent with findings from Sahoo et al. (2023), who reported genetically similar strains exhibiting diverse antibiotic resistance profiles in the river water [39]. Interestingly, the variation in (GTG)<sub>5</sub> patterns among isolates did not strongly correlate with the presence of resistance or virulence genes. The river catchment areas serve as an ideal environment for the transfer of genetic material both within and between the bacterial species. Among the CRKP isolates examined for susceptibility, 90% exhibited the MDR phenotype, while the remaining isolates were categorized as XDR. The MDR isolates have been identified in various rivers worldwide, including India (75.62%) [40], South China (87.5%) [41], and Nigeria (65.8%) [42]. Results observed in our study also corroborated with Chaturvedi et al. (2021), who observed the highest frequency of isolates resistant to  $\beta$ -lactams, cephalosporins, and sulfonamides groups of

antibiotics in Indian river systems [40]. This is likely linked to the frequent prescription of these medications in the treatment of nosocomial infections in India, owing to their clinical efficacy and low toxicity [43]. High concentrations of these antibiotics are released from hospital effluents into the river, potentially facilitating multi-drug resistance in river water isolates [44]. The CRKP isolates exhibited over 65% resistance to aminoglycosides, fluoroquinolones, tetracycline, and phenicol groups. Several investigations have also reported the high occurrence of resistance to these antibiotics in environmental isolates [40, 45, 46]. The MAR index > 0.2 for our sites aligns with the findings of Chaturvedi et al. (2020) in the Ganga river, indicating a pronounced risk of antibiotic pollution in the river system [47]. Together, these insights emphasize the necessity to tackle and mitigate the growing threat of antibiotic pollution in Indian rivers.

We observed the co-existence of carbapenemases and ESBLs in the CRKP isolates, which is in agreement with a previous study conducted by Zhang et al. (2020) in hospital sewage, treated effluents, and receiving rivers in China [48]. The high prevalence of *bla*<sub>NDM</sub> (68.13%) in the CRKP isolates has also been identified in several Indian rivers, Mutha and Ganga, as well as Ter and Ebro rivers in Spain [49]. ESBL genes have also been detected in the Yamuna River in New Delhi [50], various water supplies in Coimbatore [51], and wastewater treatment plant effluents in Ireland [52]. This coexistence of carbapenemases and ESBLs in the MDR and XDR CRKP isolates is indicative of the increasing threat posed by these bacterial infections in the community. Moreover, the absence or point mutations in genes encoding OMPs (*ompK35*, *ompK36*, and *ompK37*) may have contributed to resistance against cefoxitin, carbapenems, ciprofloxacin, and chloramphenicol antibiotics in the CRKP isolates [53].

In addition to MDR and XDR phenotype, the CRKP isolates in our study also harbored several virulence genes. The prevalence of *fimH* (type 1 Fimbriae) and *mrkD* (type 2 Fimbriae) responsible for attachment to host mucosal surfaces and the development of infection [54] was found in 41.75% and 43.95% of the isolates, respectively. Similarly, *magA* encoding for capsular polysaccharides was observed in both wastewater and river water, whereas K2 capsular serotype was found only in wastewater. These findings align closely with Barati et al. (2016), who observed a similar frequency of these virulence genes in the Matang mangrove estuary [55]. The predominant VF identified in CRKP isolates was siderophore *ybtS* (84.61%), which plays a crucial role in chelating iron from the host and inhibiting host immune defenses [56]. This finding aligns with the results of Rolbiecki et al. (2021), who observed *ybtS* as the most commonly occurring siderophore in environmental CRKP isolates [57]. The *iucA* gene, responsible for aerobactin synthesis and a key component in siderophore production in some hypervirulent strains, was detected in 54.94% of CRKP isolates [58, 59]. The isolates

from both river water (C3, C5, and D4) and wastewater (C2, C4, and D2) contained the *iroB* genes encoding salmochelin, a laboratory marker for accurately identifying hypervirulent *K. pneumoniae* [60]. The *magA* gene encoding for capsular polysaccharides was observed in isolates from both wastewater (C2, C4, and D2) and river water, whereas K2 capsular serotype was only found in wastewater. These genes are mostly responsible for higher resistance to phagocytosis and lead to metastatic septic complications [61]. In addition, 48.35% of CRKP isolates from both wastewater and river water harbored *peg344*, a metabolite transporter responsible for increased RNA abundance when grown in human ascites [62]. Based on existing literature, isolates possessing aerobactin (*iucA*) along with any of the hypermucoid phenotype genes (*magA*, K2, and *rmpA*) are considered potentially hypervirulent [57, 63]. In our study, we found that 20% ( $n = 19$ ) of CRKP isolates from wastewater (C2, C4, and D2) and river water (C3 and C5) harbored both *magA* and *iucA* genes. Although we did not perform phenotypic confirmation for hypervirulence, the presence of these genotypic markers suggests their potential for heightened virulence. These genotypic profiles indicate the possible emergence of strains with both resistance and virulence traits.

Multidrug-resistant (MDR) and hypervirulent pathotypes of *K. pneumoniae* (hvKp) were earlier believed to be distinct, with the MDR phenotype mostly linked to classical *K. pneumoniae* strains, and hvKp exhibiting lower antibiotic resistance [64, 65]. However, recent reports on MDR-hvKp strains suggest an association between antibiotic resistance and hypervirulence, raising concerns over severe infections among both immunocompromised and healthy individuals due to limited treatment options [66]. In our study, a positive association between the MAR index and virulence index was observed at sites C2, C3, C5, D1, D2, and D4 [67, 68], whereas an inverse association occurred at sites D3 and C4 [69]. Both indices are used to approximate the burden of antibiotic resistance and pathogenicity and therefore serve as proxy indicators of health risk. Nonetheless, such association studies may signal sites that warrant closer surveillance. Given the potential for these CRKP isolates harboring MDR and virulence genes to enter human populations via contaminated water, proper wastewater treatment prior to their discharge into river systems is essential to prevent their spread in aquatic environments. Several strategies have been reported for effective ARG removal, including anaerobic–aerobic treatment reactors, activated sludge processes, membrane bioreactors, constructed wetlands, and various disinfection techniques such as ozone treatment, chlorination, and UV radiation [70]. Additionally, innovative approaches involving nanomaterials, coagulation, biochar, and clay-based absorbent have shown promise in reducing the release of heavy metals and antibiotic-resistant bacteria into aquatic ecosystems [70, 71]. Furthermore, stringent

industrial regulations and antibiotic stewardship programs should be implemented to ensure routine monitoring of industrial effluents before their discharge into river systems and minimize the indiscriminate use of antibiotics, thereby mitigating the emergence of resistant strains. Collaborative efforts between environmental and public health agencies are imperative to establish integrated frameworks aimed at addressing these risks and ensuring sustainable actions to protect public health and environmental integrity.

Besides antibiotics, heavy metals have the potential to exert a sustained selection pressure, hence facilitating the persistence of ARGs [72]. Co-selection of heavy metals has been a concern for decades, and several studies have also observed that contamination with heavy metals may have a substantial impact on the dissemination of antibiotic resistance across various habitats [11, 73, 74]. In this study, we observed a notable correlation between heavy metals (As, Cd, Cr, Mn, Pb) and resistance genes including *bla*<sub>OXA-48</sub>, *bla*<sub>TEM</sub>, and *bla*<sub>SHV</sub>, suggesting that heavy metals may play a substantial role in facilitating the spread of ARGs [75]. Results from this study showed that *bla*<sub>TEM</sub> has a strong positive correlation with As (Spearman's correlation,  $p < 0.05$ ) suggesting a potential association between heavy metal concentrations and ARG distribution. The RDA ( $p = 0.034$ ) model further supported this association, indicating that heavy metals collectively explained a statistically significant portion of the variance in ARGs. These findings highlight the importance of considering both water metal concentrations and ARG abundance when assessing the environmental risks for antibiotic resistance [76]. Previous studies have reported similar patterns, where arsenic exposure showed increased resistance patterns and enhanced horizontal transfer of ARGs in isolates [77, 78].

Our previous research by Sahoo et al. (2023) also observed significant correlations between ARGs specifically *bla*<sub>TEM</sub> and heavy metals As, Cd, and Pb [39]. Although these associations do not establish causation, they align with previously proposed mechanisms that may link heavy metal exposure to increased ARG abundance, such as activation of the SOS response and alterations in cell membrane permeability [79]. According to Li et al. (2021), the persistence and spread of ARGs can be facilitated by heavy metals, whether present in high or low concentrations [80]. A similar study reported by Palm et al. (2008) demonstrated that metals directly trigger the selection of tetracycline resistance genes, including *tetA*, *tetC*, and *tetG* [81]. These genes encode proteins that function as part of an efflux pump system, thereby facilitating resistance through the active extrusion of tetracycline from bacterial cells. Recent transcriptomic analyses of hexavalent chromium-stressed MDR *E. coli* and antibiotic-susceptible *E. coli* ATCC25922 revealed a notably higher expression of ARGs, insertion sequences, DNA

and RNA methyltransferases, and toxin-antitoxin systems in MDR *E. coli* compared to control [82]. These findings underscore the adaptive transcriptional responses in MDR strains under heavy metal stress, highlighting their potential role in enhancing survival and resistance mechanisms. Therefore, while our findings suggest a correlation between heavy metals and ARGs, further mechanistic studies are needed to confirm a direct role of heavy metals in resistance proliferation [75]. Our composite risk analysis suggested that site D2 had the highest composite risk score (0.735) followed by C2 (0.699). Notably, although site C2 had a moderate chemical risk of 0.537, the overall risk was primarily driven by the presence of CRKP, contributing to the highest biological risk (0.861) in the site. Site C1 had no detectable biological risk and a lowest composite chemical risk (0.008) resulting in a composite risk score of 0.004. This suggests that site C1 is relatively uncontaminated with minimal contribution from chemical and biological hazards. The distribution of composite risk scores in several sites such as D2, C2, and C3 suggests that both chemical and biological risks contribute substantially to the overall risk. The observed correlation between chemical and biological risks demonstrates the utility of an integrated composite scoring framework for environmental risk assessment. This could further aid in the identification of hotspots for site-specific monitoring strategies. The sites with higher composite scores could be prioritized for frequent sampling to identify source contamination, which can help wastewater treatment facilities adopt advanced disinfection technologies to reduce the contamination load. Furthermore, collaborative efforts can be undertaken by the Pollution Control Board and stakeholders in implementing upstream source control measures, such as pretreatment of industrial and hospital effluents, drainage management, etc. However, despite its utility, temporal fluctuations and lack of direct linkage to health outcomes are the major constraints. The linear regression analysis indicated that 46% of the variability in composite biological risk can be explained by the presence of heavy metals. The moderate  $R^2$  value may reflect the limited sample size or the influence of other environmental variables in contributing to AMR. While earlier studies from our group identified a metal-ARG association, our composite scoring advances this understanding by demonstrating how these interactions may amplify the overall risk in specific locations. This holistic perspective may serve as a foundation for future environmental surveillance programs in assessing environmental health risk in river systems.

## Conclusion and Future Research Directions

In this study, we estimated the concentration of heavy metals in river waters and evaluated the health risks posed by its exposure through ingestion and dermal contact. The heavy metal risk assessment showed that the river water from Kathajodi (C3), Kuakhai (C5), and Daya (D3 and D4) is unfit for domestic as well as farming purposes. The presence of As and Mn in river water poses significant environmental pollution and non-carcinogenic health risks. The hazard indices of heavy metals were found to be higher for children compared to adults. In addition, the high prevalence of MDR and XDR CRKP isolates in the river water raises concern. The CRKP isolates from wastewater are the major carriers of antibiotic resistance and hypervirulence determinants, and their improper discharge into the river water results in a high incidence of these strains in the river system. In addition, the heavy metals were found to correlate with ARGs. To comprehensively assess the combined impact of chemical and biological risk, we developed a composite risk score that could aid in future environmental surveillance and targeted mitigation efforts.

While the study sheds light on the prevalence and dissemination of CRKP isolates from wastewater to river, the non-carcinogenic risk posed by heavy metals, and the correlation of heavy metals and ARGs, improvements to this study are worth considering. A more comprehensive health risk assessment, including exposure assessment, dose-response evaluation, and risk characterization, is essential to have a complete understanding of the potential public health impact. Future research should include mechanistic studies on the co-selection of heavy metals and ARGs and a detailed phenotypic characterization of hvKp strains from the environment.

**Supplementary Information** The online version contains supplementary material available at <https://doi.org/10.1007/s00248-025-02562-9>.

**Acknowledgements** The authors are grateful to Prof (Dr.) S.C. Si, Dean, Centre for Biotechnology, and Prof (Dr.) M.R. Nayak, President, Siksha 'O' Anusandhan University, for providing infrastructure and encouragement.

**Author Contributions** P.P.S.- conceptualization, designing, experimentation, formal analysis and interpretation of data, validation, visualization, investigation, writing-original draft, writing-review and editing, E.S.—resources, R.K.S.—conceptualization, supervision, fund acquisition, resources, data interpretation, validation and writing-review and editing.

**Funding** Open access funding provided by Siksha 'O' Anusandhan (Deemed To Be University). This work was supported by the University Grants Commission, New Delhi, India (Grant number 523/2020(BSR) to Siksha O Anusandhan Deemed to be University, Bhubaneswar).

**Data Availability** No datasets were generated or analysed during the current study.

## Declarations

**Competing interests** The authors declare no competing interests.

**Open Access** This article is licensed under a Creative Commons Attribution-NonCommercial-NoDerivatives 4.0 International License, which permits any non-commercial use, sharing, distribution and reproduction in any medium or format, as long as you give appropriate credit to the original author(s) and the source, provide a link to the Creative Commons licence, and indicate if you modified the licensed material. You do not have permission under this licence to share adapted material derived from this article or parts of it. The images or other third party material in this article are included in the article's Creative Commons licence, unless indicated otherwise in a credit line to the material. If material is not included in the article's Creative Commons licence and your intended use is not permitted by statutory regulation or exceeds the permitted use, you will need to obtain permission directly from the copyright holder. To view a copy of this licence, visit <http://creativecommons.org/licenses/by-nc-nd/4.0/>.

## References

- Wei J, Duan M, Li Y, Nwankwegu AS, Ji Y, Zhang J (2019) Concentration and pollution assessment of heavy metals within surface sediments of the Raohe Basin. *China Sci Rep* 9:13100. <https://doi.org/10.1038/s41598-019-49724-7>
- Ngweme GN, Atibu EK, Al Salah DMM, Muanamoki PM, Kiyombo GM, Mulaji CK et al (2020) Heavy metal concentration in irrigation water, soil and dietary risk assessment of *Amaranthus viridis* grown in peri-urban areas in Kinshasa, Democratic Republic of the Congo. *Watershed Ecol Environ* 2:16–24. <https://doi.org/10.1016/j.wsee.2020.07.001>
- Chen J, Li J, Zhang H, Shi W, Liu Y (2019) Bacterial heavy-metal and antibiotic resistance genes in a copper tailing dam area in Northern China. *Front Microbiol* 10. <https://doi.org/10.3389/fmicb.2019.01916>
- Rahman Z, Singh VP (2018) Assessment of heavy metal contamination and Hg-resistant bacteria in surface water from different regions of Delhi. *India Saudi J Biol Sci* 25:1687–1695. <https://doi.org/10.1016/j.jsbs.2016.09.018>
- Shen F, Mao L, Sun R, Du J, Tan Z, Ding M (2019) Contamination evaluation and source identification of heavy metals in the sediments from the Lishui River watershed, Southern China. *Int J Environ Res Public Health* 16:336. <https://doi.org/10.3390/ijerph16030336>
- Hafiz TA, Alanazi S, Alghamdi SS, Mubarak MA, Aljabr W, Madkhali N et al (2023) *Klebsiella pneumoniae* bacteraemia epidemiology: resistance profiles and clinical outcome of King Fahad Medical City isolates, Riyadh. *Saudi Arabia BMC Infect Dis* 23:579. <https://doi.org/10.1186/s12879-023-08563-8>
- Shon AS, Russo TA (2012) Hypervirulent *Klebsiella pneumoniae*: the next superbug? *Future Microbiol* 7:669–671. <https://doi.org/10.2217/fmb.12.43>
- Holt KE, Wertheim H, Zadoks RN, Baker S, Whitehouse CA, Dance D et al (2015) Genomic analysis of diversity, population structure, virulence, and antimicrobial resistance in *Klebsiella pneumoniae*, an urgent threat to public health. *Proc Natl Acad Sci* 112. <https://doi.org/10.1073/pnas.1501049112>
- Loudermilk EM, Kotay SM, Barry KE, Parikh HI, Colosi LM, Mathers AJ (2022) Tracking *Klebsiella pneumoniae* carbapenemase gene as an indicator of antimicrobial resistance dissemination from a hospital to surface water via a municipal wastewater treatment plant. *Water Res* 213:118151. <https://doi.org/10.1016/j.watres.2022.118151>
- Jamil M, Malook I, Rehman SU, Aslam MM, Fayyaz M, Shah G et al (2024) Inoculation of heavy metal resistant bacteria alleviated heavy metal-induced oxidative stress biomarkers in spinach (*Spinacia oleracea* L.). *BMC Plant Biol* 24:221. <https://doi.org/10.1186/s12870-024-04757-7>
- Mazhar SH, Li X, Rashid A, Su J, Xu J, Brejnrod AD et al (2021) Co-selection of antibiotic resistance genes, and mobile genetic elements in the presence of heavy metals in poultry farm environments. *Sci Total Environ* 755:142702. <https://doi.org/10.1016/j.scitotenv.2020.142702>
- Gupta S, Graham DW, Sreekrishnan TR, Ahammad SZ (2023) Heavy metal and antibiotic resistance in four Indian and UK rivers with different levels and types of water pollution. *Sci Total Environ* 857:159059. <https://doi.org/10.1016/j.scitotenv.2022.159059>
- Samreen, Ahmad I, Malak HA, Abulreesh HH (2021) Environmental antimicrobial resistance and its drivers: a potential threat to public health. *J Glob Antimicrob Resist* 27:101–111. <https://doi.org/10.1016/j.jgar.2021.08.001>
- Iskandar K, Molinier L, Hallit S, Sartelli M, Hardcastle TC, Haque M et al (2021) Surveillance of antimicrobial resistance in low- and middle-income countries: a scattered picture. *Antimicrob Resist Infect Control* 10:63. <https://doi.org/10.1186/s13756-021-00931-w>
- Mishra N (2025) Kanas gastroenteritis outbreak in Odisha is due to river water pollution. *New Indian Express*. [https://www.newindianexpress.com/cities/bhubaneswar/2025/Jan/24/kanas-gastroenteritis-outbreak-in-odisha-is-due-to-river-water-pollution?utm\\_source=izooto&utm\\_medium=push\\_notifications&utm\\_campaign=recover-abandoned-tab&utm\\_content=notification1](https://www.newindianexpress.com/cities/bhubaneswar/2025/Jan/24/kanas-gastroenteritis-outbreak-in-odisha-is-due-to-river-water-pollution?utm_source=izooto&utm_medium=push_notifications&utm_campaign=recover-abandoned-tab&utm_content=notification1). Accessed 24 Jan 2025
- Mishra R (2025) 'Diarrhoea' deaths: daya river water highly polluted, not fit for human consumption, says Puri CDMO. *ODISHA BYTES*. <https://odishabytes.com/diarrhoea-deaths-daya-river-highly-polluted-not-fit-for-human-consumption-says-puri-cdmo/>. Accessed 20 Jan 2025
- APHA (2012) Standard methods for the examination of water and wastewater, 22nd edition edited by E. W. Rice, R. B. Baird, A. D. Eaton and L. S. Clesceri. 22nd ed. Washington, D.C., USA: American Public Health Association (APHA), American Water Works Association (AWWA) and Water Environment Federation (WEF)
- EPA (2015) Updated ambient water quality criteria for the protection of human health. United States environmental protection agency. <https://www.epa.gov/wqc/human-health-water-quality-criteria-and-methods-toxics>. Accessed 20 Jan 2025
- Bureau of Indian Standards (2012) Indian standard drinking water specification (IS 10500: 2012). BIS, New Delhi, India.
- Pobi KK, Nayek S, Gope M, Rai AK, Saha R (2020) Sources evaluation, ecological and health risk assessment of potential toxic metals (PTMs) in surface soils of an industrial area. *India Environ Geochem Health* 42:4159–4180. <https://doi.org/10.1007/s10653-020-00517-2>
- Hussain J, Dubey A, Hussain I, Arif M, Shankar A (2020) Surface water quality assessment with reference to trace metals in River Mahanadi and its tributaries. *India Appl Water Sci* 10:193. <https://doi.org/10.1007/s13201-020-01277-1>
- EPA (2004) National Recommended Water Quality Criteria. United States Environ Prot Agency. <https://doi.org/10.1201/9781420032963.axb>
- Xiao R, Guo D, Ali A, Mi S, Liu T, Ren C et al (2019) Accumulation, ecological-health risks assessment, and source

- apportionment of heavy metals in paddy soils: a case study in Hanzhong, Shaanxi. *China Environ Pollut* 248:349–357. <https://doi.org/10.1016/j.envpol.2019.02.045>
24. Wang Y, Lu J, Zhang S, Li J, Mao L, Yuan Z et al (2021) Non-antibiotic pharmaceuticals promote the transmission of multidrug resistance plasmids through intra- and intergenera conjugation. *ISME J* 15:2493–2508. <https://doi.org/10.1038/s41396-021-00945-7>
  25. Wang G, Liu H-Q, Gong Y, Wei Y, Miao A-J, Yang L-Y et al (2017) Risk assessment of metals in urban soils from a typical industrial city, Suzhou, Eastern China. *Int J Environ Res Public Health* 14:1025. <https://doi.org/10.3390/ijerph14091025>
  26. Sahoo RK, Das A, Gaur M, Pattanayak A, Sahoo S, Debata NK et al (2019) Genotypic validation of extended-spectrum  $\beta$ -lactamase and virulence factors in multidrug resistance *Klebsiella pneumoniae* in an Indian hospital. *Pathog Glob Health* 113:315–321. <https://doi.org/10.1080/20477724.2019.1705020>
  27. Kaboré B, Ouédraogo GA, Cissé H, Ouédraogo HS, Sampo E, Zongo KJ et al (2022) (GTG)5-PCR fingerprinting of multidrug resistant *Escherichia coli* bacteria isolates from hospital in Ouagadougou. *Burkina Faso BMC Microbiol* 22:118. <https://doi.org/10.1186/s12866-022-02537-7>
  28. Das A, Sahoo RK, Gaur M, Dey S, Sahoo S, Sahu A et al (2022) Molecular prevalence of resistance determinants, virulence factors and capsular serotypes among colistin resistance carbapenemase producing *Klebsiella pneumoniae*: a multi-centric retrospective study. *3 Biotech* 12. <https://doi.org/10.1007/s13205-021-03056-4>
  29. Basak S, Singh P, Rajurkar M (2016) Multidrug resistant and extensively drug resistant bacteria: a study. *J Pathog* 2016:1–5. <https://doi.org/10.1155/2016/4065603>
  30. Singh SK, Ekka R, Mishra M, Mohapatra H (2017) Association study of multiple antibiotic resistance and virulence: a strategy to assess the extent of risk posed by bacterial population in aquatic environment. *Environ Monit Assess* 189:320. <https://doi.org/10.1007/s10661-017-6005-4>
  31. Adefisoye MA, Okoh AI (2016) Identification and antimicrobial resistance prevalence of pathogenic *Escherichia coli* strains from treated wastewater effluents in Eastern Cape. *South Africa Microbiologyopen* 5:143–151. <https://doi.org/10.1002/mbo3.319>
  32. Singh G, Chaudhary S, Gupta D, Kumar MV (2024) Assessing the water quality of River Ganga in Varanasi, India, through WQI, NPI, and multivariate techniques: a comprehensive study. *Water Pract Technol* 19:1099–1118. <https://doi.org/10.2166/wpt.2024.027>
  33. Yu H, Zhang J, Yin Z, Liu Z, Chen J, Xu J et al (2024) A method for quantifying the contribution of algal sources to CODMn in water bodies based on ecological chemometrics and its potential applications. *J Environ Chem Eng* 12:111943. <https://doi.org/10.1016/j.jece.2024.111943>
  34. Joshi A, Mishra S (2017) Anthropocene effects on the river Daya and the lagoon Chilika by the effluents of Bhubaneswar city India: a physico-chemical study. *Int J Adv Res* 5:1370–84. <https://doi.org/10.21474/IJAR01/5656>
  35. Patel P, Raju NJ, Reddy BCSR, Suresh U, Sankar DB, Reddy TVK (2018) Heavy metal contamination in river water and sediments of the Swarnamukhi River Basin, India: risk assessment and environmental implications. *Environ Geochem Health* 40:609–623. <https://doi.org/10.1007/s10653-017-0006-7>
  36. Eid MH, Eissa M, Mohamed EA, Ramadan HS, Tamás M, Kovács A et al (2024) New approach into human health risk assessment associated with heavy metals in surface water and groundwater using Monte Carlo Method. *Sci Rep* 14:1008. <https://doi.org/10.1038/s41598-023-50000-y>
  37. Saha N, Rahman MS, Ahmed MB, Zhou JL, Ngo HH, Guo W (2017) Industrial metal pollution in water and probabilistic assessment of human health risk. *J Environ Manage* 185:70–78. <https://doi.org/10.1016/j.jenvman.2016.10.023>
  38. Alidadi H, Tavakoly Sany SB, Zarif Garaati Oftadeh B, Mohamad T, Shamszade H, Fakhari M (2019) Health risk assessments of arsenic and toxic heavy metal exposure in drinking water in north-east Iran. *Environ Health Prev Med* 24:59. <https://doi.org/10.1186/s12199-019-0812-x>
  39. Sahoo S, Sahoo RK, Gaur M, Behera DU, Sahu A, Das A, et al (2023) Urban wastewater contributes to the emergence of carbapenem-resistant *Klebsiella pneumoniae* (CRKP) in an urban receiving river in eastern India. *Lett Appl Microbiol* 76. <https://doi.org/10.1093/lambio/ovac005>
  40. Chaturvedi P, Chowdhary P, Singh A, Chaurasia D, Pandey A, Chandra R et al (2021) Dissemination of antibiotic resistance genes, mobile genetic elements, and efflux genes in anthropogenically impacted riverine environments. *Chemosphere* 273:129693. <https://doi.org/10.1016/j.chemosphere.2021.129693>
  41. Su H-C, Ying G-G, Tao R, Zhang R-Q, Zhao J-L, Liu Y-S (2012) Class 1 and 2 integrons, sul resistance genes and antibiotic resistance in *Escherichia coli* isolated from Dongjiang River. *South China Environ Pollut* 169:42–49. <https://doi.org/10.1016/j.envpol.2012.05.007>
  42. Obayiuwana A, Ogunjobi A, Yang M, Ibekwe M (2018) Characterization of bacterial communities and their antibiotic resistance profiles in wastewaters obtained from pharmaceutical facilities in Lagos and Ogun States, Nigeria. *Int J Environ Res Public Health* 15:1365. <https://doi.org/10.3390/ijerph15071365>
  43. Van Boeckel TP, Gandra S, Ashok A, Caudron Q, Grenfell BT, Levin SA et al (2014) Global antibiotic consumption 2000 to 2010: an analysis of national pharmaceutical sales data. *Lancet Infect Dis* 14:742–750. [https://doi.org/10.1016/S1473-3099\(14\)70780-7](https://doi.org/10.1016/S1473-3099(14)70780-7)
  44. Korzeniewska E, Harnisz M (2013) Beta-lactamase-producing Enterobacteriaceae in hospital effluents. *J Environ Manage* 123:1–7. <https://doi.org/10.1016/j.jenvman.2013.03.024>
  45. Kotlarska E, Łuczkiewicz A, Pisowacka M, Burzyński A (2015) Antibiotic resistance and prevalence of class 1 and 2 integrons in *Escherichia coli* isolated from two wastewater treatment plants, and their receiving waters (Gulf of Gdansk, Baltic Sea, Poland). *Environ Sci Pollut Res* 22:2018–2030. <https://doi.org/10.1007/s11356-014-3474-7>
  46. Pazda M, Kumirska J, Stepnowski P, Mulkiewicz E (2019) Antibiotic resistance genes identified in wastewater treatment plant systems – a review. *Sci Total Environ* 697:134023. <https://doi.org/10.1016/j.scitotenv.2019.134023>
  47. Chaturvedi P, Chaurasia D, Pandey A, Gupta P (2020) Co-occurrence of multidrug resistance,  $\beta$ -lactamase and plasmid mediated AmpC genes in bacteria isolated from river Ganga, northern India. *Environ Pollut* 267:115502. <https://doi.org/10.1016/j.envpol.2020.115502>
  48. Zhang L, Ma X, Luo L, Hu N, Duan J, Tang Z et al (2020) The prevalence and characterization of extended-spectrum  $\beta$ -lactamase- and carbapenemase-producing bacteria from hospital sewage, treated effluents and receiving rivers. *Int J Environ Res Public Health* 17:1183. <https://doi.org/10.3390/ijerph17041183>
  49. Singh R, Singh AP, Kumar S, Giri BS, Kim K-H (2019) Antibiotic resistance in major rivers in the world: a systematic review on occurrence, emergence, and management strategies. *J Clean Prod* 234:1484–1505. <https://doi.org/10.1016/j.jclepro.2019.06.243>
  50. Bajaj P, Singh NS, Kanaujia PK, Virdi JS (2015) Distribution and molecular characterization of genes encoding CTX-M and AmpC  $\beta$ -lactamases in *Escherichia coli* isolated from an Indian urban aquatic environment. *Sci Total Environ* 505:350–356. <https://doi.org/10.1016/j.scitotenv.2014.09.084>
  51. Natarajan K, Subashkumar R (2017) Incidence of multi drug resistance and diversity of TEM-1 Beta lactamase in gram

- negative bacteria isolated from clinical and environmental sample. *Int J Appl Sci Biotechnol* 5:302–308. <https://doi.org/10.3126/ijasbt.v5i3.17693>
52. Smyth C, O'Flaherty A, Walsh F, Do TT (2020) Antibiotic resistant and extended-spectrum  $\beta$ -lactamase producing faecal coliforms in wastewater treatment plant effluent. *Environ Pollut* 262:114244. <https://doi.org/10.1016/j.envpol.2020.114244>
  53. Indrajith S, Mukhopadhyay AK, Chowdhury G, Farraj DAA, Alkufeydi RM, Natesan S et al (2021) Molecular insights of Carbapenem resistance *Klebsiella pneumoniae* isolates with focus on multidrug resistance from clinical samples. *J Infect Public Health* 14:131–8. <https://doi.org/10.1016/j.jiph.2020.09.018>
  54. Struve C, Bojer M, Krogfelt KA (2008) Characterization of *Klebsiella pneumoniae* type 1 fimbriae by detection of phase variation during colonization and infection and impact on virulence. *Infect Immun* 76:4055–4065. <https://doi.org/10.1128/IAI.00494-08>
  55. Barati A, Ghaderpour A, Chew LL, Bong CW, Thong KL, Chong VC, et al (2016) Isolation and characterization of aquatic-borne *Klebsiella pneumoniae* from tropical estuaries in Malaysia. *Int J Environ Res Public Health* 13. <https://doi.org/10.3390/ijerph13040426>
  56. Han R, Niu M, Liu S, Mao J, Yu Y, Du Y (2022) The effect of siderophore virulence genes *entB* and *ybtS* on the virulence of Carbapenem-resistant *Klebsiella pneumoniae*. *Microb Pathog* 171:105746. <https://doi.org/10.1016/j.micpath.2022.105746>
  57. Rolbiecki D, Harnisz M, Korzeniewska E, Buta M, Hubeny J, Zieliński W (2021) Detection of carbapenemase-producing, hypervirulent *Klebsiella* spp. in wastewater and their potential transmission to river water and WWTP employees. *Int J Hyg Environ Health* 237. <https://doi.org/10.1016/j.ijheh.2021.113831>
  58. Russo TA, Shon AS, Beanan JM, Olson R, MacDonald U, Pomakov AO et al (2011) Hypervirulent *K. pneumoniae* secretes more and more active iron-acquisition molecules than “classical” *K. pneumoniae* thereby enhancing its virulence. *PLoS One* 6:e26734. <https://doi.org/10.1371/journal.pone.0026734>
  59. Wu J, Chen J, Wang Y, Meng Q, Zhao J (2022) Siderophore *iucA* of hypermucoviscous *Klebsiella pneumoniae* promotes liver damage in mice by inducing oxidative stress. *Biochem Biophys Reports* 32:101376. <https://doi.org/10.1016/j.bbrep.2022.101376>
  60. Russo TA, Olson R, Fang C-T, Stoesser N, Miller M, MacDonald U, et al (2018) Identification of biomarkers for differentiation of hypervirulent *klebsiella pneumoniae* from classical *K. pneumoniae*. *J Clin Microbiol* 56. <https://doi.org/10.1128/JCM.00776-18>
  61. Yeh K-M, Kurup A, Siu LK, Koh YL, Fung C-P, Lin J-C et al (2007) Capsular Serotype K1 or K2, Rather than *magA* and *rmpA*, is a major virulence determinant for *klebsiella pneumoniae* liver abscess in Singapore and Taiwan. *J Clin Microbiol* 45:466–471. <https://doi.org/10.1128/JCM.01150-06>
  62. Bulger J, MacDonald U, Olson R, Beanan J, Russo TA (2017) Metabolite transporter PEG344 is required for full virulence of hypervirulent *Klebsiella pneumoniae* strain hvKP1 after pulmonary but not subcutaneous challenge. *Infect Immun* 85. <https://doi.org/10.1128/IAI.00093-17>
  63. Liu C, Guo J (2019) Hypervirulent *Klebsiella pneumoniae* (hypermucoviscous and aerobactin positive) infection over 6 years in the elderly in China: antimicrobial resistance patterns, molecular epidemiology and risk factor. *Ann Clin Microbiol Antimicrob* 18. <https://doi.org/10.1186/s12941-018-0302-9>
  64. Bialek-Davenet S, Criscuolo A, Ailloud F, Passet V, Jones L, Delannoy-Vieillard A-S et al (2014) Genomic definition of hypervirulent and multidrug-resistant *Klebsiella pneumoniae* clonal groups. *Emerg Infect Dis* 20:1812–1820. <https://doi.org/10.3201/eid2011.140206>
  65. Wyres KL, Wick RR, Judd LM, Froumine R, Tokolyi A, Gorrie CL et al (2019) Distinct evolutionary dynamics of horizontal gene transfer in drug resistant and virulent clones of *Klebsiella pneumoniae*. *PLOS Genet* 15:e1008114. <https://doi.org/10.1371/journal.pgen.1008114>
  66. Tang M, Kong X, Hao J, Liu J (2020) Epidemiological characteristics and formation mechanisms of multidrug-resistant hypervirulent *Klebsiella pneumoniae*. *Front Microbiol* 11. <https://doi.org/10.3389/fmicb.2020.581543>
  67. Sahly H, Navon-Venezia S, Roesler L, Hay A, Carmeli Y, Podschun R et al (2008) Extended-spectrum  $\beta$ -lactamase production is associated with an increase in cell invasion and expression of fimbrial adhesins in *Klebsiella pneumoniae*. *Antimicrob Agents Chemother* 52:3029–3034. <https://doi.org/10.1128/AAC.00010-08>
  68. Wyres KL, Nguyen TNT, Lam MMC, Judd LM, van Vinh CN, Dance DAB et al (2020) Genomic surveillance for hypervirulence and multi-drug resistance in invasive *Klebsiella pneumoniae* from South and Southeast Asia. *Genome Med* 12:11. <https://doi.org/10.1186/s13073-019-0706-y>
  69. Fernandes R, Abreu R, Serrano I, Such R, Garcia-Vila E, Quirós S et al (2024) Resistant *Escherichia coli* isolated from wild mammals from two rescue and rehabilitation centers in Costa Rica: characterization and public health relevance. *Sci Rep* 14:8039. <https://doi.org/10.1038/s41598-024-57812-6>
  70. Barancheshme F, Munir M (2018) Strategies to combat antibiotic resistance in the wastewater treatment plants. *Front Microbiol* 8. <https://doi.org/10.3389/fmicb.2017.02603>
  71. Mukhopadhyay R, Drigo B, Sarkar B (2024) Mitigation potential of antibiotic resistance genes in water and soil by clay-based adsorbents. *Npj Mater Sustain* 2:26. <https://doi.org/10.1038/s44296-024-00030-y>
  72. Knapp CW, McCluskey SM, Singh BK, Campbell CD, Hudson G, Graham DW (2011) Antibiotic resistance gene abundances correlate with metal and geochemical conditions in archived scottish soils. *PLoS ONE* 6:e27300. <https://doi.org/10.1371/journal.pone.0027300>
  73. Imran M, Das KR, Naik MM (2019) Co-selection of multi-antibiotic resistance in bacterial pathogens in metal and microplastic contaminated environments: an emerging health threat. *Chemosphere* 215:846–857. <https://doi.org/10.1016/j.chemosphere.2018.10.114>
  74. Pal C, Bengtsson-Palme J, Kristiansson E, Larsson DGJ (2015) Co-occurrence of resistance genes to antibiotics, biocides and metals reveals novel insights into their co-selection potential. *BMC Genomics* 16:964. <https://doi.org/10.1186/s12864-015-2153-5>
  75. Ohore OE, Addo FG, Zhang S, Han N, Anim-Larbi K (2019) Distribution and relationship between antimicrobial resistance genes and heavy metals in surface sediments of Taihu Lake. *China J Environ Sci* 77:323–335. <https://doi.org/10.1016/j.jes.2018.09.004>
  76. Knapp CW, Callan AC, Aitken B, Shearn R, Koenders A, Hinwood A (2017) Relationship between antibiotic resistance genes and metals in residential soil samples from Western Australia. *Environ Sci Pollut Res* 24:2484–2494. <https://doi.org/10.1007/s11356-016-7997-y>
  77. Kothari A, Kumar P, Gaurav A, Kaushal K, Pandey A, Yadav SRM et al (2023) Association of antibiotics and heavy metal arsenic to horizontal gene transfer from multidrug-resistant clinical strains to antibiotic-sensitive environmental strains. *J Hazard Mater* 443:130260. <https://doi.org/10.1016/j.jhazmat.2022.130260>

78. Ahmed N, Tahir K, Aslam S, Cheema SM, Rabaan AA, Turkistani SA et al (2022) Heavy Metal (Arsenic) Induced antibiotic resistance among extended-spectrum  $\beta$ -lactamase (ESBL) producing bacteria of nosocomial origin. *Pharmaceuticals* 15:1426. <https://doi.org/10.3390/ph15111426>
79. Zhang S, Wang Y, Song H, Lu J, Yuan Z, Guo J (2019) Copper nanoparticles and copper ions promote horizontal transfer of plasmid-mediated multi-antibiotic resistance genes across bacterial genera. *Environ Int* 129:478–487. <https://doi.org/10.1016/j.envint.2019.05.054>
80. Li Y, Chen H, Song L, Wu J, Sun W, Teng Y (2021) Effects on microbiomes and resistomes and the source-specific ecological risks of heavy metals in the sediments of an urban river. *J Hazard Mater* 409:124472. <https://doi.org/10.1016/j.jhazmat.2020.124472>
81. Palm GJ, Lederer T, Orth P, Saenger W, Takahashi M, Hillen W et al (2008) Specific binding of divalent metal ions to tetracycline and to the Tet repressor/tetracycline complex. *JBIC J Biol Inorg Chem* 13:1097–1110. <https://doi.org/10.1007/s00775-008-0395-2>
82. Zeng X, Cao Y, Wang L, Wang M, Wang Q, Yang Q (2023) Viability and transcriptional responses of multidrug resistant *E. coli* to chromium stress. *Environ Pollut* 324:121346. <https://doi.org/10.1016/j.envpol.2023.121346>

**Publisher's Note** Springer Nature remains neutral with regard to jurisdictional claims in published maps and institutional affiliations.